Weakly Guiding Fibers

D. Gloge

Thin glass fibers imbedded into a glass cladding of slightly lower refractive index represent a promising medium for optical communication. This article presents simple formulas and functions for the fiber parameters as a help for practical design work. It considers the propagation constant, mode delay, the cladding field depth, and the power distribution in the fiber cross section. Plots vs frequency of these parameters are given for 70 modes

I. Introduction

Recently, glass fibers have been produced that permit the transmission of optical signals over several kilometers.[1] In general, these fibers support many modes, which propagate at different velocities.[2] Since this causes signal distortion over long distances, fibers that transmit only a limited number of modes are of special interest.[3] A fiber waveguide consists of a thin central glass core surrounded by a glass cladding of slightly lower refractive index. Most modes can be suppressed by making the core thin and the index different between core and cladding small.[3] Typically, a difference of a few parts in a thousand is feasible. This avoids propagation of most modes. The modes that do propagate are weakly guided, but in general the guidance is sufficient to negotiate bends with radii of tens of centimeters.[4]

Maxwell's equations have exact solutions for the dielectric cylinder,[2] but even with the simplifying assumption that the cladding be infinitely thick these solutions are too complicated to be evaluated without computer. Recent efforts in simplifying the theory for weakly guided modes had promising results,[5] but in the region of interest, they did not lead to the kind of simple formulas one would wish to have for fiber design work. The following paper is aimed at such formulas and functions. It is meant as a help for engineering applications directed toward fiber communication systems. Most results are valid for all frequencies and propagation conditions—even at cutoff—with an accuracy of the order of the index difference between core and cladding.

The author is with Bell Telephone Laboratories, Inc., Crawford Hill Laboratory, Holmdel, New Jersey 07733.

Received 28 May 1971.

II. Mode Parameters and Characteristic Equation

Consider the cylindric core of radius a depicted in Fig. 1(a). The refractive index of the core is n_c. Let the cladding material of index n extend to infinity. We shall use both cartesian coordinates (x,y) and cylindrical coordinates (r,ϕ). The propagation constant β of any mode of this fiber is limited within the interval $n_c k \geq \beta \geq nk$, where $k = 2\pi/\lambda$ is the wavenumber in free space. If we define parameters

$$u = a(k^2 n_c^2 - \beta^2)^{\frac{1}{2}} \tag{1}$$

$$w = a(\beta^2 - k^2 n^2)^{\frac{1}{2}}, \tag{2}$$

the mode field can be expressed by Bessel function $J(ur/a)$ inside the core and modified Hankel function $K(wr/a)$ outside the core. The quadratic summation

$$v^2 = u^2 + w^2 \tag{3}$$

leads to a third parameter,

$$v = ak(n_c^2 - n^2)^{\frac{1}{2}}, \tag{4}$$

which can be considered as a normalized frequency. By matching the fields at the core–cladding interface, we obtain characteristic functions $u(v)$ or $w(v)$ for every mode; the propagation constant and all other parameters of interest can be derived from these functions.

For weak guidance, we have

$$\Delta = (n_c - n)/n \ll 1. \tag{5}$$

In this case, we can construct modes whose transverse field is essentially polarized in one direction. This can be deduced from the results of Ref. 5, but in order to elucidate the approximation involved, let us try a direct derivation. We postulate transverse field components

$$E_y = H_x \begin{Bmatrix} Z_0/n_c \\ Z_0/n \end{Bmatrix} = E_l \begin{Bmatrix} J_l(ur/a)/J_l(u) \\ K_l(wr/a)/K_l(w) \end{Bmatrix} \cos l\phi. \tag{6}$$

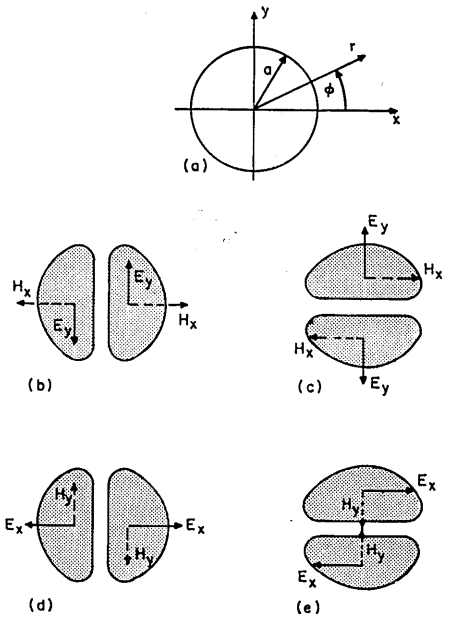

Fig. 1. Sketch of the fiber cross section and the four possible distributions of LP_{11}.

Here, as in the following, the upper line holds for the core and the lower line for the cladding; Z_0 is the plane wave impedance in vacuum, and E_l the electrical field strength at the interface. Figure 1(b)–(e) illustrate the case $l = 1$. Since we have the freedom of choosing $\sin l\phi$ or $\cos l\phi$ in Eq. (6) and two orthogonal states of polarization, we can construct a set of four modes for every l as long as $l > 0$. For $l = 0$, we have only a set of two modes polarized orthogonally with respect to each other.

The longitudinal components can be obtained from the equations[6]

$$E_z = \frac{iZ_0}{k}\begin{Bmatrix} 1/n_c^2 \\ 1/n^2 \end{Bmatrix}\frac{\partial H_x}{\partial y}, \tag{7a}$$

and

$$H_z = (i/kZ_0)(\partial E_y/\partial x). \tag{7b}$$

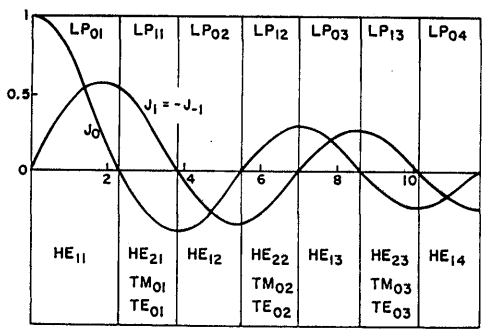

Fig. 2. The regions of the parameter u for modes of order $l = 0,1$.

By introducing Eq. (6), we therefore have

$$E_z = \frac{-iE_l}{2ka}\left\{\begin{aligned} &\frac{u}{n_c}\frac{J_{l+1}(ur/a)}{J_l(u)}\sin(l+1)\phi \\ &\quad + \frac{u}{n_c}\frac{J_{l-1}(ur/a)}{J_l(u)}\sin(l-1)\phi \\ &\frac{w}{n}\frac{K_{l+1}(wr/a)}{K_l(w)}\sin(l+1)\phi \\ &\quad - \frac{w}{n}\frac{K_{l-1}(wr/a)}{K_l(w)}\sin(l-1)\phi \end{aligned}\right\}, \tag{8a}$$

$$H_z = \frac{-iE_l}{2kZ_0a}\left\{\begin{aligned} &u\frac{J_{l+1}(ur/a)}{J_l(u)}\cos(l+1)\phi \\ &\quad - u\frac{J_{l-1}(ur/a)}{J_l(u)}\cos(l-1)\phi \\ &w\frac{K_{l+1}(wr/a)}{K_l(w)}\cos(l+1)\phi \\ &\quad + w\frac{K_{l-1}(wr/a)}{K_l(w)}\cos(l-1)\phi \end{aligned}\right\}. \tag{8b}$$

For small Δ, the longitudinal components [Eqs. (8a), (8b)] are small compared to the transverse components. The factors involved are u/ak and w/ka which because of Eqs. (1) and (2) are both of the order $\Delta^{\frac{1}{2}}$. Repeated differentiation of Eqs. (8a) and (8b) leads to transverse components which are not identical with the postulated field [Eq. (6)] but small of order Δ compared to it. We shall neglect these fields in the following. It is this approximation that determines the accuracy of our assumption of linearly polarized modes.

To match the fields at the interface let us write Eq. (6) in terms of cylindrical components. We then have

$$E_\phi = \frac{1}{2}E_l\begin{Bmatrix} J_l(ur/a)/J_l(u) \\ K_l(wr/a)/K_l(w) \end{Bmatrix}[\cos(l+1)\phi + \cos(l-1)\phi], \tag{9a}$$

$$H_\phi = -\frac{1}{2}\frac{E_l}{Z_0}\begin{Bmatrix} n_c J_l(ur/a)/J_l(u) \\ nK_l(wr/a)/K_l(w) \end{Bmatrix} \times [\sin(l+1)\phi - \sin(l-1)\phi]. \tag{9b}$$

If we set $n_c = n$ in Eqs. (8) and (9) and use the recurrence relations for J_l and K_l, we can match all tangential field components at the interface by the one equation

$$u[J_{l-1}(u)/J_l(u)] = -w[(K_{l-1}(w)/K_l(w)]. \tag{10}$$

This is the characteristic equation for the linearly polarized (LP) modes. Setting $w = 0$ yields the cutoff values $J_{l-1}(u) = 0$. For $l = 0$, this includes the roots of the Bessel function $J_{-1}(u) = -J_1(u)$, which we shall count so as to include $J_1(0) = 0$ as the first root. We then obtain the cutoff values indicated in Fig. 2 for LP_{0m} and LP_{1m}. In the limit of $w \to \infty$, we have $J_l(u) = 0$. Thus, the solutions for u are between the zeros of $J_{l-1}(u)$ and $J_l(u)$. Every solution is associated with one set of modes designated LP_{lm}. For $l \geq 1$, each set comprises four modes.

The accuracy of the characteristic equation can be improved if we retain n and n_c as different in Eqs. (8)

and (9). In this case, however, terms with $(l + 1)\phi$ and $(l - 1)\phi$ satisfy two different characteristic equations:

$$(u/n_r)[J_{l\pm1}(u)/J_l(u)] = \pm(w/n)[K_{l\pm1}(w)/K_l(w)]. \quad (11)$$

By using the recurrence relations for J_l and K_l, one can easily show that these two equations converge into Eq. (10) for $n_c = n$. For $n_c \neq n$, this degeneracy ceases to exist; each mode LP_{lm} breaks up into modes with terms $(l + 1)\phi$, which can be identified as $HE_{l+1,m}$, and modes with terms $(l - 1)\phi$ which form $EH_{l-1,m}$ or TE_m and TM_m.[2,5] This association is indicated in the lower half of Fig. 2 for the cases $l = 0$ or 1. A more rigorous proof of the previous results is given in the Appendix, where Eqs. (10) and (11) are derived directly from the exact characteristic equation. The following calculations are based on Eq. (10), which is found to be sufficiently accurate for most practical applications.

III. Approximate Analytic Solution

By using Eq. (3) and differentiating both sides of Eq. (10) with respect to v, one can write the characteristic Eq. (10) in the form[5]

$$du/dv = (u/v)[1 - \kappa_l(w)], \quad (12)$$

where

$$\kappa_l(w) = K_l^2(w)/K_{l-1}(w)K_{l+1}(w). \quad (13)$$

For large w, we have $\kappa_l \approx 1 - (1/v)$. This can be used to solve Eq. (12) for large v.[5] Unfortunately, parameters of interest like the propagation constant or the field depth in the cladding depend on the difference $v^2 - u^2$. As this difference becomes small in the region of interest, the relative error introduced by the above approximation becomes intolerably large. To be useful, an approximation of u must improve toward smaller v.

With this in mind, we replace Eq. (13) by

$$\kappa_l \approx 1 - (w^2 + l^2 + 1)^{-\frac{1}{2}}, \quad (14)$$

which not only approximates Eq. (13) for large w, but provides a reasonable fit throughout. We now use Eq. (3) and replace w^2 by $v^2 - u^2$. Yet since u stays in the narrow region between successive roots of adjacent Bessel functions, we may write

$$w \approx (v^2 - u_c^2)^{\frac{1}{2}}, \quad (15)$$

replacing u by its cutoff value u_c. For the mode LP_{lm}, u_c is the mth root of $J_{l-1}(u)$. The approximations (14) and (15) are satisfactory for all modes except $LP_{01} = HE_{11}$, whose mode parameters u, v, and w all approach zero simultaneously.

If we exclude HE_{11}, we can now use Eqs. (14), (15), and the boundary value u_c at cutoff to solve Eq. (12). The result is

$$u(v) = u_c \exp[\arcsin(s/u_c) - \arcsin(s/v)]/s, \quad (16)$$

with

$$s = (u_c^2 - l^2 - 1)^{\frac{1}{2}}. \quad (17)$$

In the case of the HE_{11} mode, a more careful approximation is necessary, although the basic approach is similar to the one outlined previously. Without going into detail, we list the result

$$u(v) = (1 + \sqrt{2})v/[1 + (4 + v^4)^{\frac{1}{4}}] \quad \text{for } HE_{11}. \quad (18)$$

We mentioned earlier that u is bound between successive zeros of the Bessel functions J_{l-1} and J_l. We thus know the asymptotic value u_∞ for $v \to \infty$ exactly. Equations (16) and (18) approximate these values within an error of 2%; this is a good indication of the accuracy of Eqs. (16) and (18). For $v \gg s$ (far enough from cutoff), we can reduce Eqs. (16) and (18) to

$$u(v) = u_\infty[1 - (1/v)] \quad (19)$$

for all modes, using the mth root of $J_l(u)$ for u_∞.

IV. Propagation Constant and Mode Delay

With the help of $u(v)$, we can calculate the propagation constant β from Eq. (1). In order to make the results independent of particular fiber configurations, however, we shall not plot β directly but the ratio

$$b(v) = 1 - (u^2/v^2) = [(\beta^2/k^2) - n^2]/(n_c^2 - n^2), \quad (20)$$

which, for small index difference, reduces to

$$b \approx [(\beta/k) - n]/(n_c - n). \quad (21)$$

From this and Eq. (5) we obtain the propagation constant

$$\beta = nk(b\Delta + 1) = nk[1 + \Delta - \Delta(u^2/v^2)]. \quad (22)$$

Since β and b are proportional, the quantity b can be understood as a normalized propagation constant. Figure 3 shows $b(v)$ for 18 LP modes. A comparison with exact computer solutions showed deviations that were too small to be displayed in Fig. 3.

Direct detection of intensity-modulated light signals recognizes dispersion effects only in the envelope of the

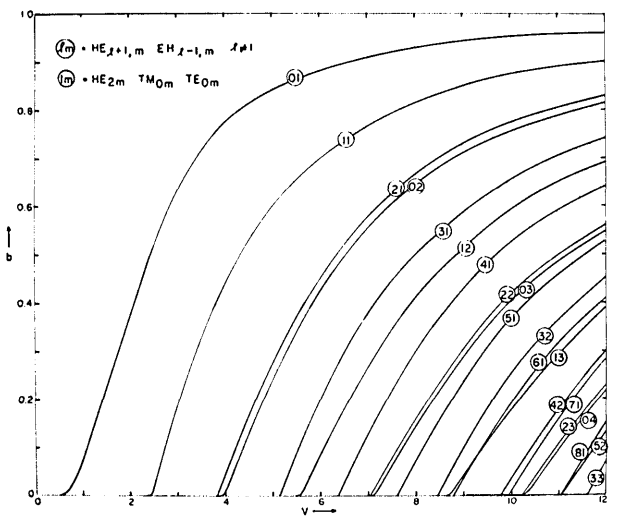

Fig. 3. Normalized propagation parameter $b = (\beta/k - n)/(n_c - n)$ as a function of the normalized frequency v.

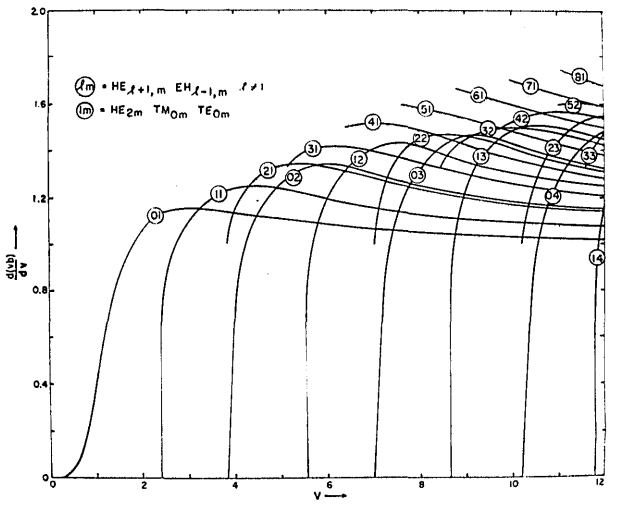

Fig. 4. Normalized group delay $d(vb)/dv$ as a function of v.

light signal. This envelope is influenced by the group delay

$$\tau_{gr} = (L/c)(d\beta/dk). \tag{23}$$

Here c is the vacuum velocity of light and L the length of the fiber. When we differentiate Eq. (22), we must consider the k dependence of n, Δ, and b. Yet, if the dispersion of the core and the cladding glass is approximately the same, Δ is independent of k. Moreover, for all glasses, $kdn/dk \ll n$. If we ignore products of Δ with $(k/n)(dn/dk)$, we obtain

$$\tau_{gr} = \frac{L}{c}\{[d(nk)/dk] + n\Delta[d(vb)/dv]\}. \tag{24}$$

The first part of Eq. (24) characterizes the material dispersion, which is the same for all modes. The second part, which represents the group delay on account of waveguide dispersion, is governed by the derivative $d(vb)/dv$. Because of Eqs. (12) and (20), this derivative can be expressed by

$$d(vb)/dv = 1 - (u/v)^2(1 - 2\kappa), \tag{25}$$

with κ from Eq. (13). This function is plotted in Fig. 4. Far from cutoff, it approaches unity for all modes. At cutoff, $d(vb)/dv = 2\kappa(0)$. This results in cutoff values $d(vb)/dv = 0$ for $l = 0$, 1, and $2[1 - (1/l)]$ for $l \geq 2$. As Fig. 4 shows, the mode of largest order l has the largest group delay. The difference between this and the slowest mode is approximately $1 - (2/l)$. For large v, we have $l_{max} \approx v$. Thus we obtain a group spread $[(1 - (2/v)](n_1 - n_2)L/c$ for a fiber that propagates many modes.

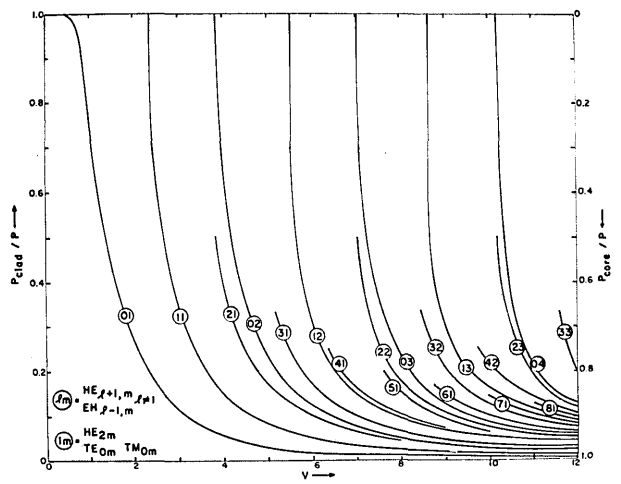

Fig. 5. Portion of the mode power which propagates in the cladding plotted vs v.

V. Power Flow and Power Density

The Poynting vector in axial direction can be calculated from the cross product of the transverse fields given in Eq. (6). Integration over the cross section of core and cladding leads to tabulated integrals[5,9]; the results are

$$P_{core} = [1 + (w^2/u^2)(1/\kappa)](\pi a^2/2)(Z_0/n_c)E_l^2 \tag{26}$$

and

$$P_{clad} = [(1/\kappa) - 1](\pi a^2/2)(Z_0/n)E_l^2 \tag{27}$$

for the power flow in core and cladding, respectively. If we ignore the small difference between n_c and n, the total power in a certain mode becomes

$$P = P_{core} + P_{clad} = (v^2/u^2)(1/\kappa)(\pi a^2/2)(Z_0/n)E_l^2. \tag{28}$$

Practical fibers have small heat and scattering losses which cause significant attenuation over long distances. In general, these losses are attributable to certain parts of the fiber and proportional to the power propagating in this part. For considerations of this kind, it is convenient to use the power fractions

$$P_{core}/P = 1 - (u^2/v^2)(1 - \kappa) \tag{29}$$

and

$$P_{clad}/P = (u^2/v^2)(1 - \kappa), \tag{30}$$

which are plotted in Fig. 5. As expected, the mode power is concentrated in the core far away from cutoff. As cutoff is approached, the power of low order modes ($l = 0,1$) withdraws into the cladding, whereas modes with $l \geq 2$ maintain a fixed ratio of $l - 1$ between the power in core and cladding at cutoff.

The power density is related to the mode power P by

$$p(r) = \kappa \frac{u^2}{v^2}\frac{2P}{\pi a^2}\left\{\begin{matrix} J_l^2(ur/a)/J_l^2(u) \\ K_l^2(wr/a)/K_l^2(w)\end{matrix}\right\}\cos^2 l\phi.$$

By averaging over ϕ at $r = a$, we obtain the mean density

$$\bar{p}(r) = \kappa(u^2/v^2)\frac{P}{\pi a^2}\left\{\begin{matrix} J_l^2(ur/a)/J_l^2(u) \\ K_l^2(wr/a)/K_l^2(w)\end{matrix}\right\}. \tag{31}$$

At the core–cladding interface, we have $r = a$ and

$$\bar{p}(a) = \kappa(u^2/v^2)(P/\pi a^2). \tag{32}$$

The normalized density $\pi a^2\bar{p}(a)/P$ is plotted in Fig. 6. For modes of order $l = 0,1$ this density approaches zero both at cutoff and far away from it, having a maxi-

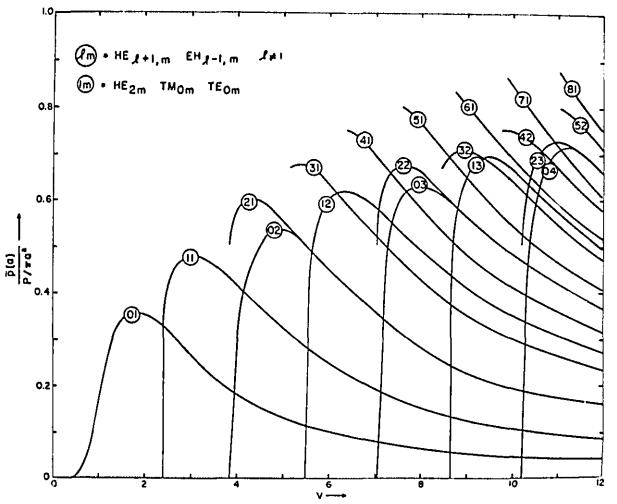

Fig. 6. Normalized power density at the core-cladding interface plotted vs v.

mum in between. Modes with $l \geq 2$ have $\bar{p}(a) = [1 - (1/l)]P/\pi a^2$ at cutoff.

For $r \gg a/w$, we can replace the K functions in Eq. (31) by their approximation for large argument and obtain

$$\bar{p}(r) \approx \kappa(u^2/v^2)(P/\pi ar) \exp[-2w(r - a)/a] \quad \text{for } r \gg a,$$

as long as w is not too small. The power density decreases exponentially with the distance from the interface. The parameter w is plotted in Fig. 7. It decreases sharply as cutoff is approached and is zero at cutoff. For sufficiently small w we may set $u = v$ and replace the K functions in Eq. (31) by their approximation for small argument, obtaining

$$\bar{p}(r) \approx \kappa_l(P/\pi a^2)(a/r)^l \quad \text{for } r > a,\ w = 0.$$

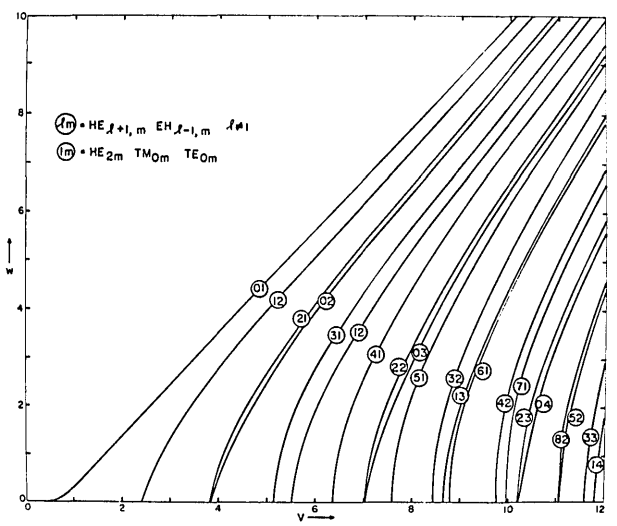

Fig. 7. Cladding parameter w plotted vs v.

This function describes the cutoff power distribution in the cladding. It decreases with the distance from the axis for all but the lowest azimuthal order, whose cladding field is independent of the radius. These results are of course based on our theoretical model of a core imbedded into an unbounded cladding.

VI. Approximations for Multimode Fibers

Fibers that transmit a large number of modes are of particular interest in connection with incoherent light sources, as, for example, light-emitting diodes. This is because the amount of light that the fiber accepts from this source increases with the number of modes it transmits. Clearly, fibers with a large mode volume neither can nor need be evaluated in as much detail as was done in previous sections. A much simpler mode picture is required. To find this, let us introduce a somewhat simpler way of counting the modes.

Figure 8 illustrates the front end of a fiber and the cone of light that this fiber accepts. The cone is limited by those rays that, after entering the front

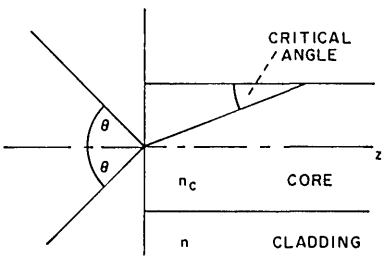

Fig. 8. Sketch of the fiber front face and the cone of light that the fiber accepts.

end of the core, are totally reflected at the interface between core and cladding. These rays form an angle

$$\theta \approx \sin\theta = (n_c^2 - n^2)^{\frac{1}{2}} \tag{33}$$

with the axis. Consider now the free-space modes which can enter the front area πa^2 of the core.[8] There are pairs of modes that are perpendicularly polarized with respect to each other. Each pair occupies a cone of solid angle $\pi\delta^2$, where[8]

$$\delta = \lambda/\pi a. \tag{34}$$

The total number of free-space modes accepted by the fiber is consequently

$$N \approx 2(\theta/\delta)^2 \tag{35}$$

or, because of Eq. (4),

$$N \approx v^2/2. \tag{36}$$

This is also the number of modes transmitted by the fiber. We find this confirmed if we count all cutoff values $u_c < v$, bearing in mind that the lowest value

represents two modes and all others four. Equation (36) permits us to label the fiber modes in the sequence of their cutoff values. Vice versa, we can predict the cutoff of the νth mode approximately at

$$u_c \approx (2\nu)^{\frac{1}{2}}. \tag{37}$$

This rule, of course, holds only for large ν.

Let us now use this counting method to describe fibers with large mode volume. We restrict ourselves to operation far from cutoff, ignoring, among the large number of modes, those few that are appreciably close to cutoff. We thus set $\kappa = 1$. We replace u by u_c, bearing in mind that the parameter u never departs much from its cutoff value u_c. Because of Eq. (20), the propagation parameter b then becomes

$$b = 1 - (u_c^2/v^2) = 1 - (\nu/N). \tag{38}$$

Equation (25) can be simplified accordingly to yield the group delay parameter

$$d(vb)/dv = 1 + (u_c^2/v^2) = 1 + (\nu/N). \tag{39}$$

We can estimate the power density at the interface by converting Eq. (32). This yields

$$\bar{p}(a) = (P/\pi a^2)(u_c^2/v^2) = (P/\pi a^2)(\nu/N). \tag{40}$$

The power flow in the cladding can be obtained from Eq. (30) by using the approximation $1 - \kappa \approx (v^2 - u_c^2)^{-\frac{1}{2}}$, which is obtained from Eq. (14). Equation (30) then reads

$$P_{\text{clad}} \approx Pu_c^2/v^2(v^2 - u_c^2)^{\frac{1}{2}} = P\nu/N(2N - 2\nu)^{\frac{1}{2}}. \tag{41}$$

The incoherent source, in general, excites every fiber mode with the same amount of power. We find the average power distribution in a fiber under these conditions by averaging Eqs. (40) and (41) over all N modes, treating the mode index ν as a continuous variable. We then obtain for the density at the interface

$$[\bar{p}(a)/P]_{\text{tot}} = \frac{1}{\pi a^2 N}\int_0^N \frac{\nu}{N}\,d\nu = \frac{1}{2\pi a^2}. \tag{42}$$

It is interesting to note that this quantity is independent of N or the parameter v. The average cladding power follows from an integration of Eq. (41). The result is

$$(P_{\text{clad}}/P)_{\text{tot}} = \frac{1}{N}\int_0^N \frac{\nu d\nu}{N(2N - 2\nu)^{\frac{1}{2}}} = \frac{4}{3}N^{-\frac{1}{2}}. \tag{43}$$

The power flow in the cladding decreases proportional to $N^{-\frac{1}{2}}$ or, because of Eq. (36), proportional to $1/v$.

As an example, consider a fiber with a core index of 1.5, $\Delta = 0.003$, and a core radius of 25 μ. This results in $v = 20.3$ at 0.9-μ wavelength. The group delay between the fastest and the slowest mode is 13.5 nsec after 1 km. The fiber transmits 206 modes. Roughly 10% of the power propagates in the cladding.

VII. Conclusions

The theory of dielectric waveguides greatly simplifies if the difference between the refractive indices of core and cladding is small. In this case, linearly polarized modes with simple fields and a simple characteristic equation can be defined. Approximate analytic solutions can be derived which are exact at cutoff, showing a maximum relative error of up to 2% for very high frequencies. The mode parameters that follow from these solutions have sufficient accuracy for most practical applications. We consider the propagation constant (Fig. 3), mode delay (Fig. 4), the cladding field depth (Fig. 7), and the power distribution in the fiber cross section (Figs. 5 and 6). Far from cutoff, the group velocity of all modes is smaller than the plane wave velocity in the core and decreases as cutoff is approached. For certain modes, however, this trend reverses shortly before cutoff is reached. The fraction of mode power that propagates in the cladding is the larger the closer the mode to cutoff. For most modes, however, it is just a small fraction of the total power even at cutoff. The modes with the two lowest azimuthal orders are an exception. Their cutoff distributions are characterized by plane wave fields in the cladding which contain practically all the mode power. In multimode fibers with incoherent input, the power is in general equally distributed among all modes. In this case, we find that the power density at the interface is independent of the number of modes, but the power flow in the cladding decreases proportional to the root of that number.

I am grateful to E. A. J. Marcatili for helpful suggestions.

Appendix: Another Derivation of the Simplified Characteristic Equations

As mentioned earlier, the problem of the dielectric cylinder with sharp index step can be solved exactly; using the nomenclature defined in Sec. II, one can write the exact characteristic equation in the form

$$(Q - D - 2\Delta\{[(l \pm 1)/\omega^2] \pm [K_l(\omega)/\omega K_{l\pm1}(\omega)]\})(Q - D) = Q^2[1 - 2\Delta(u^2/v^2)], \tag{A1}$$

where

$$Q = (l \pm 1)(v^2/u^2w^2), \tag{A2}$$

$$D = [J_l(u)/uJ_{l\pm1}(u)] \mp [K_l(w)/wK_{l\pm1}(w)], \tag{A3}$$

and

$$2\Delta = (n_c^2 - n^2)/n_c^2. \tag{A4}$$

The upper sign holds for HE_{l+1} modes and the lower sign for EH_{l-1}, TM, and TE. Equation (A4) agrees with Eq. (5) in the case of small index differences $n_c - n$. If Δ is set to zero in Eq. (A1), we find $D = 0$; Eq. (A3) then becomes the simplified characteristic Eq. (10). For small Δ, D is also small. Let us now simplify Eq. (A1) to the extent that we retain terms linear in Δ or D. This results in

$$D = \Delta\{Q(u^2/v^2) - [(l \pm 1)/w^2] \mp [K_l(w)/wK_{l\pm1}(w)]\} \tag{A5}$$

and with Eq. (A2)

$$D = \mp\Delta[K_l(w)/wK_{l\pm1}(w)]. \tag{A6}$$

By introducing this into Eq. (A3) and inserting Eq. (5), we find

$$(u/n_c)[J_{l\pm1}(u)/J_l(u)] = \pm(w/n)[K_{l\pm1}(w)/K_l(w)]. \quad \text{(A7}$$

This is exactly the characteristic Eq. (11).

References

1. F. P. Kapron, D. B. Keck, and R. D. Maurer, Appl. Phys. Lett. **17**, 423 (1970).
2. E. Snitzer, J. Opt. Soc. Am. **51**, 491 (1961).
3. K. C. Kao and G. A. Hockham, Proc. IEE **113**, 1151 (1966).
4. E. A. J. Marcatili, Bell Syst. Tech. J. **48**, 2103 (1969).
5. A. W. Snyder, IEEE Trans. Microwave Theory Techniques **MTT-17**, 1130 (1969).
6. S. A. Schelkunoff, *Electromagnetic Waves* (Van Nostrand, New York, 1943), p. 94.
7. A. W. Snyder, IEEE Trans. Microwave Theory Techniques **MTT-17**, 1138 (1969).
8. G. Toraldo di Francia, J. Opt. Soc. Am. **59**, 799 (1969).
9. P. Moon and D. E. Spencer, *Field Theory Handbook* (Springer, Berlin, 1961), p. 192.